

Alkali flame ionization detector for gas chromatography using an alkali salt aerosol as the enhancement source

Eric D. Conte and Eugene F. Barry*

Department of Chemistry, University of Massachusetts Lowell, Lowell, MA 01854 (USA)

(First received January 29th, 1993; revised manuscript received April 6th, 1993)

ABSTRACT

A new design of an alkali flame ionization detector (AFID) is presented and differs from other configurations in that the enhancement source is introduced as an aerosol into a flame ionization detector (FID) rather than as a stationary solid bead positioned above a FID flame. This aerosol enters the detector as a hydrogen flame located perpendicular to the FID jet. Because the present design permits a constant and fresh supply of alkali salt to reach the detector, detector response does not fatigue over time. This AFID design also allows for operation as a FID by implementing a simple pneumatic procedure. This paper will deal with the performance and optimization of the detector in the phosphorous mode. The linear range for triethylphosphate exceeds four orders of magnitude. Selectivity ratios are in the four orders of magnitude range and detection limits for organophosphorus compounds studied ranged from 2.38 to 14.2 pg P/s.

INTRODUCTION

The earliest version of the alkali flame ionization detector (AFID) [1,2] dates back to 1964. In these initial designs an alkali salt was placed on the collector electrode and heated by a conventional flame. For phosphorus-containing compounds, the sensitivity of response increased by approximately two orders of magnitude compared to the FID, although a drawback was unreproducible response. The lifetime of the alkali source was limited by its volatilization which resulted in detector instability and gradual fatigue in response. Further improvements in detector design have been reported by Coahran and others [3–8] who positioned a compacted form of the alkali salt upon the FID jet. Unfortunately, this configuration where the alkali salt was placed in a concentric manner around the FID jet resulted in the same problems of limited lifetime and instability as the initial design.

In an alternative design, known as the flameless alkali sensitized detector (FASD), reported by Kolb and Bischoff [9], the alkali salt compacted in a more stable glass bead was ionized electrically above the FID flame. Additional designs involving electrical heating [10–14] have been reported. These designs offered improved performance in comparison with the earlier designs, but exhibited decreased sensitivity over time and necessitated frequent replacement of exhausted alkali salt sources.

The enhancement mechanism is not well understood, although mechanisms have been suggested [9,15,16] where nitrogen and phosphorus compounds are converted into free radicals during their elution into the flame. The free radicals are transformed into organic anions by the donation of electrons from alkali atoms (Li, Na, K, Rb and Cs) through either a solid- or gas-phase process. The ion current that is formed through this operation is responsible for the observed signal enhancement.

The proposed aerosol arrangement described in this paper circumvents several of these earlier

* Corresponding author.

problems including source replacement and gradually fatiguing response over time by providing a constant introduction of the alkali salt through ultrasonic generation. Previous work using a pneumatic alkali salt design on packed columns was performed in our laboratory [17]. The selectivity ratios, detection limits and optimization parameters of this detector in the phosphorus mode are discussed for organophosphorus pesticides.

EXPERIMENTAL

Materials

The pesticides used in the study include parathion (99% purity), diazinon (99%), chlorpyrifos (99.9%), malathion (98.5%) (ChemService, West Chester, PA, USA) while azinophosmethyl (99%) and methyl parathion (99.8%) were supplied by the Environmental Protection Agency, Research Triangle Park, NC, USA. Reagent-grade triethylphosphate and tributylphosphate were obtained from Eastman Kodak, Rochester, NY, USA whereas hexamethylphosphoramide, triethylphosphonoacetate, and penta-decane were acquired from Aldrich, Milwaukee, WI, USA. Organophosphorus standard solutions were prepared in reagent grade acetone at the following concentrations: phorate (4.23 $\mu\text{g}/\text{l}$), disulfoton (6.30 $\mu\text{g}/\text{l}$), tetraethylpyrophosphate (TEPP) (4.02 $\mu\text{g}/\text{l}$), parathion (6.09 $\mu\text{g}/\text{l}$), dimethoate (3.92 $\mu\text{g}/\text{l}$) and methyl parathion (7.08 $\mu\text{g}/\text{l}$). Solvents used to dissolve the phosphorus compounds were carbon tetrachloride, methylene chloride and *n*-hexane (J.T. Baker, Phillipsburg, NJ, USA), *n*-tetradecane (Aldrich) and cyclohexane (Alltech, Deerfield, IL, USA). Reagent-grade alkali salts employed for aerosol generation were potassium chloride, cesium chloride (J.T. Baker), rubidium chloride, sodium chloride (Fisher Scientific, Pittsburgh, PA, USA) and lithium chloride (Mallinckrodt, St. Louis, MO, USA).

Instrumentation

The gas chromatographic system was a Model 5890A (Hewlett-Packard, Avondale, PA, USA) equipped with a split/splitless injector. An HP-1 fused-silica capillary column, 30 m \times 0.25 mm

I.D., film thickness 0.25 μm , was utilized for all separations. The injector and detector temperatures were maintained at 220°C; helium was employed as carrier gas and operated at a linear velocity of 23 cm/s. The detector signal was filtered through a resistance-capacitance (RC) circuit having a time constant of 1.03 s and processed by an IBM-compatible computer (Model ZW-248-82; Zenith Data Systems, Benton Harbor, MI, USA) using Lab Calc software (Galactic Industries, Salem, NH, USA). All chromatograms were digitally smoothed using Savitsky-Golay five-point smoothing.

Glass-ware apparatus

The glass-ware apparatus used for aerosol generation is depicted in Fig. 1 where an inverted 250-ml erlenmeyer flask (b) was positioned to initially contain the aerosol produced from a home ultrasonic humidifier (a) (Model 691-100, Sunbeam, Hattiesburg, MS, USA). On the mouth of the flask was placed a 10 cm \times 10 cm polystyrene film (c) which was secured by silicon adhesive. Two glass tubes were

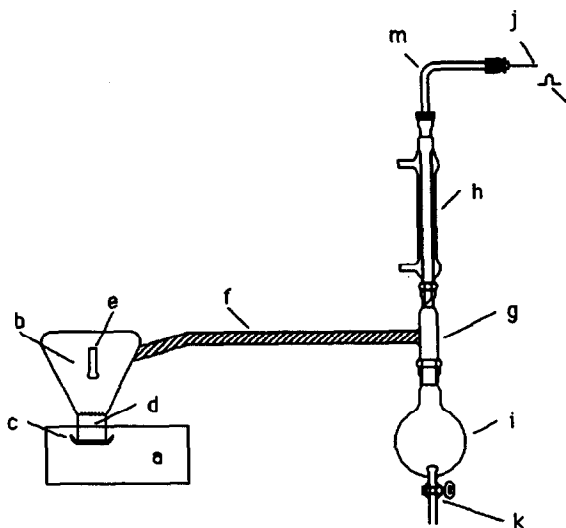


Fig. 1. AFID glass-ware apparatus. a = Ultrasonic nebulizer; b = 250-ml erlenmeyer flask; c = polystyrene film; d = alkali salt solution; e = hydrogen and nitrogen gas inlet; f = outlet tube for desolvation system wrapped in heating tape; g = T-joint adapter; h = condensation tube; i = 35-ml round-bottom flask; j = alkali flame jet; k = stopcock; l = FID jet; m = tube connecting condensation tube with alkali flame tip.

attached to the flask. The first tube (e) (50 mm \times 3 mm I.D.) to which was connected the flame-support hydrogen and nitrogen flow streams and a second tube (f) (240 mm \times 10 mm I.D.) 90° to the other tube contained the heated aerosol stream. This latter tube exiting the flask was fitted with a T adapter (g) which connected a condensation tube (h) (Wheaton, cat. No. 333970) and a 35-ml round-bottom flask (i) to collect condensate. Tube f was wrapped with heating tape to maintain the temperature at 110°C. A stopcock (k) was installed on the round bottom flask to facilitate removal of condensate. An additional tube (m) (80 mm \times 7 mm I.D.) was connected to the top of the condensation tube allowing a direct path to the detector through the use of a 1/4 in. (1 in. = 2.54 cm) plastic nut and a stainless-steel 1/4 to 1.16 in. reducing anion at the end of which was connected a stainless-steel tube (j) (30 mm \times 0.71 mm I.D.). The stainless-steel tube (j) is located perpendicular to the FID jet (l) in the detector chamber and is used as the alkali metal salt flame jet as illustrated in Fig. 2.

The original HP detector base was replaced with one fabricated from brass (n) [60 mm

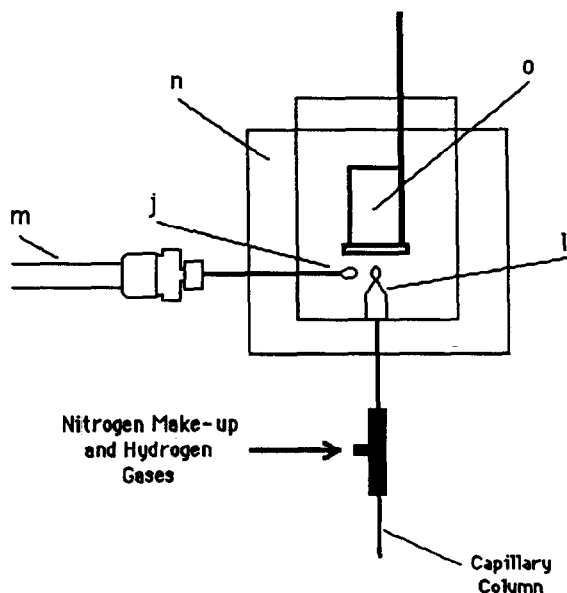


Fig. 2. Schematic diagram of the AFID. j = alkali flame jet; l = FID jet; m = tube connecting condensation tube with alkali flame tip; n = detector base; o = collector electrode.

(length) \times 40 mm (width) \times 40 mm (height)] into which holes were drilled to accommodate the alkali flame jet (10 mm \times 3 mm), (8 mm) for the FID jet, (1 mm) air, (1 mm) for the electrical ground of the FID jet, (2 mm) for the temperature thermocouple, and (10 mm) for the detector heater cartridge. The end of the capillary column was inserted at a position 1 mm below the tip of the FID jet. A stainless-steel 1/8 in. Swagelok T was used to modify existing flow channels which permitted hydrogen and nitrogen make-up gas to enter the FID jet. The collector electrode, which was composed of a 24 mm diameter aluminum disk, the heater, thermocouple, and FID jet were all connected to the existing electronic modules of the gas chromatograph.

RESULTS AND DISCUSSION

A solution containing 36.5 ng P/ μ l triethylphosphate in hexane was used for phosphorus optimization. With a 2- μ l injection and a column split ratio of 142:1 a final analyte mass of 0.51 ng P reached the TID. Optimization graphs for five detector gases are presented in Figs. 3 and 4. For the alkali aerosol flame, nitrogen and hydrogen gases were used to optimize two variables, the flame temperature and the amount of aerosol swept to the detector. These two gases were found to yield the optimal signal response at flow-rates of 90 ml/min and 47 ml/min for nitrogen and hydrogen, respectively. For the

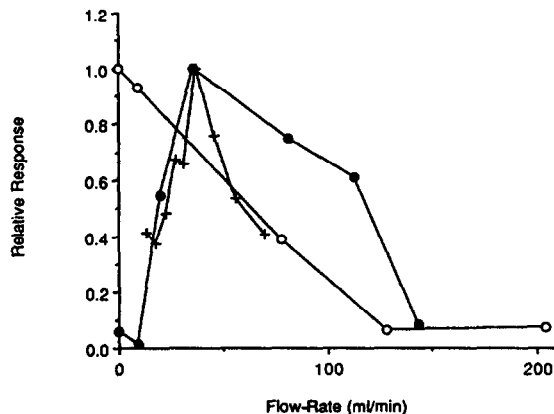


Fig. 3. FID hydrogen (+), make-up (●), and air (○) flow-rate optimizations.

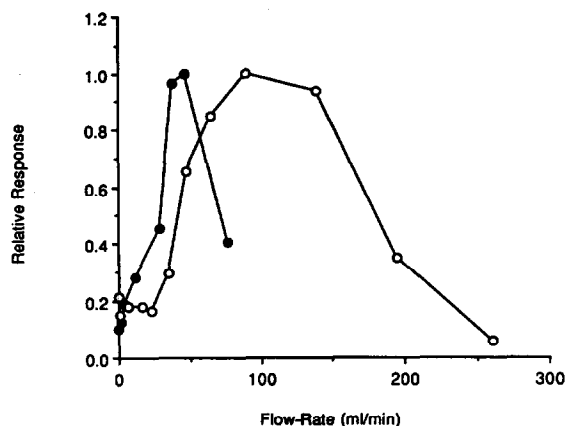


Fig. 4. Alkali nitrogen (○) and alkali hydrogen (●) flow-rate optimizations.

FID jet, the make-up flow (nitrogen) was optimized at 36 ml/min while the flow of hydrogen was optimized at 38 ml/min. Because both flames were housed in a single detector assembly, a single supply of air was used as the oxidant. A flow-rate of 0 ml/min produced the maximum peak response. This need for a rich flame is demonstrated by noting increasing response with decreasing air flow-rate. Because the detector is not a completely closed system, atmospheric oxygen is the sole contributor to flame support. The vertical gap between the flame jets and the horizontal displacement of the flame jets relative to each other were optimized at 3 mm and 5 mm, respectively, as shown in Fig. 5. Optimum response was also noted when the alkali flame jet, being electrically neutral, was positioned to be in direct contact with the collector electrode. Distinct flame formations attached to the orifice of each flame jet were observed when the collector electrode was removed.

The effect of introducing 100 $\mu\text{g/ml}$ aqueous solutions of CsCl, RbCl, KCl, LiCl, and NaCl on detector response was investigated. As displayed in Fig. 6, maximum response is associated with KCl and decreases with increasing molecular mass. The effect of varying KCl concentration from 0 to 1000 $\mu\text{g/ml}$ on selectivity was also explored and is illustrated in Fig. 7 for a separation of malathion and parathion in cyclohexane. The condensation tube maintained at 0°C elimi-

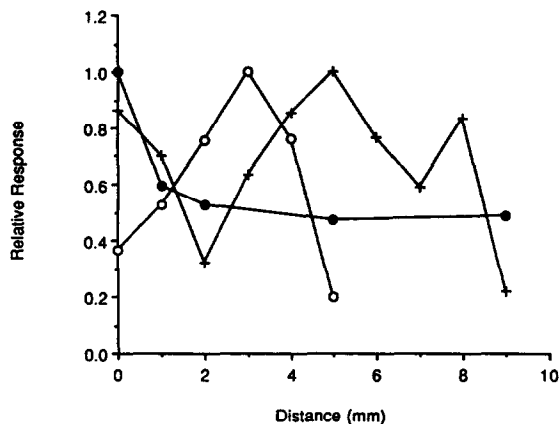


Fig. 5. Detector flame and collector distances optimization. Horizontal displacement distance of the flames (+), vertical gap distance of the flames (○) and collector distance from alkali flame jet (●).

nated the possibility of leaching and subsequent transport of alkali vapors into the alkali flame jet. Decreasing response for cyclohexane with increasing salt concentration is observed along with the high selectivity of the phosphorus-containing analytes. A concentration of 400 $\mu\text{g/ml}$ KCl created the problem of coating the collector electrode with a fine layer of salt over time and thus creating an unstable baseline. However, a concentration of 100 $\mu\text{g/ml}$ KCl completely alleviated this problem with no significant deposition of salt on the FID jet or collector electrode.

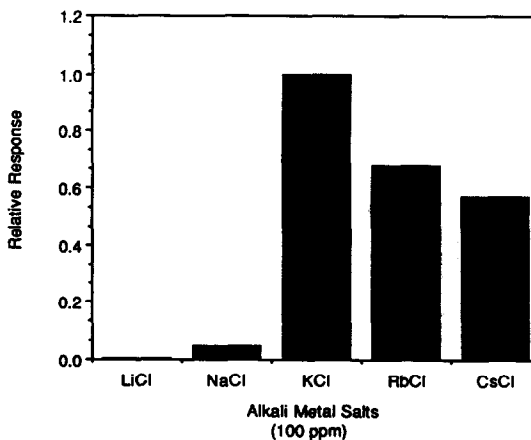


Fig. 6. Alkali salt optimization. ppm = $\mu\text{g/ml}$.

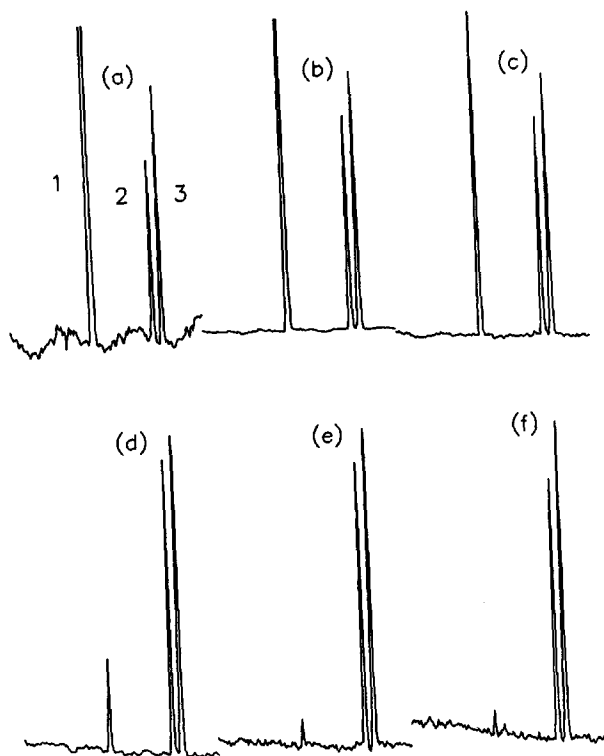


Fig. 7. Effect of KCl concentration. Peaks: 1 = cyclohexane; 2 = parathion 2.67 ng P; 3 = malathion 2.31 ng P. KCl concentrations: (a) blank, (b) 400 ng/ml, (c) 4.00 μ g/ml, (d) 40.0 μ g/ml, (e) 400 μ g/ml, (f) 1000 μ g/ml. GC conditions: column temperature, 150°C; split ratio of 150:1; 2- μ l injection.

Detection limits, linearity and selectivity

Minimum detectable mass rates were determined by dividing three times the standard deviation of the baseline noise by the slope of the calibration curve and the analyte peak at half-height. The standard deviation of the noise is given by $s_B = N_{p-p}/r$, where N_{p-p} is the peak-to-peak noise and r is 5 for random Gaussian noise [18]. Minimum detectable mass rates for five organophosphorus pesticides are presented in Table I and range from 2.38 pg P/s for disulfoton to 14.2 pg P/s for dimethoate. Detector linearity was approximately 4.5 orders of magnitude determined with triethylphosphate as the solute. The separation of six organophosphorus pesticides at the low nanogram level is displayed in Fig. 8.

In Table II selectivity ratios for various or-

TABLE I
MINIMUM DETECTABLE MASS RATE (MDMR) OF SELECTED ORGANOPHOSPHORUS PESTICIDES

Compound	MDMR (pg P/s)
Disulfoton	2.38
Phorate	2.81
Parathion	5.29
Methyl parathion	11.7
Dimethoate	14.2

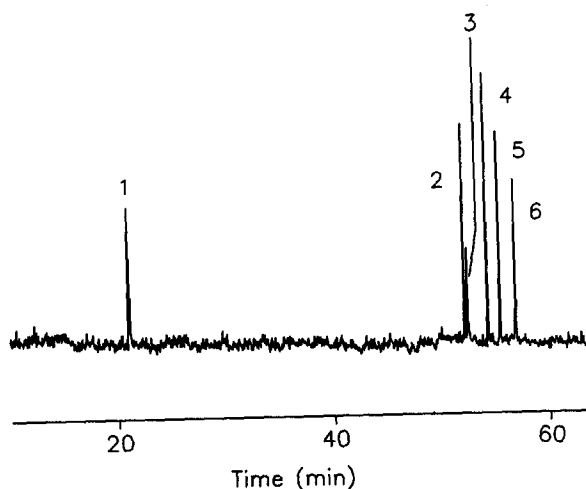


Fig. 8. Separation of an organophosphorus pesticide mixture with AFID detection. Peaks: 1 = TEPP 1.23 ng P; 2 = phorate 0.80 ng P; 3 = dimethoate 0.76 ng P; 4 = disulfoton 1.02 ng P; 5 = methyl parathion 1.29 ng P; 6 = parathion 0.92 ng P. GC conditions: column temperature: 50°C (1 min), 2°C/min to 140°C (10 min), 10°C/min to 240°C (8 min); split ratio of 3:1; 2- μ l injection.

TABLE II
SELECTIVITY RATIOS OF SELECTED ORGANOPHOSPHORUS COMPOUNDS

Compound	Selectivity ratio (g P/g C)
Hexamethylphosphoamide	10 700
Malathion	20 400
Methyl parathion	25 400
Chlorpyrifos	26 800
Parathion	32 700
Tributylphosphate	35 200
Azinphosmethyl	39 000
Triethylphosphonoacetate	73 200

ganophosphorus species are presented, which all fall in the 10^4 range. The ratios were obtained by calculating the ratio of the organophosphorus compound response per mass unit of phosphorus to the ratio of tetradecane response per mass unit of carbon. The effect of chlorinated solvents on contamination of the alkali source, known to decrease the sensitivity of nitrogen–phosphorus detectors, was also explored. An alkali salt introduced in aerosol form circumvents this situation. Repetitive one microliter injections which corresponded to 16 ng of phorate and 21 ng of parathion in carbon tetrachloride were made to monitor detector stability over a 9-h period at 15-min intervals. Peak areas of phorate and parathion were compared and found to be constant and suggests no evidence of decreased sensitivity due to contamination.

Applications

This detector design also permits one to revert detector operation back to a FID by sim-

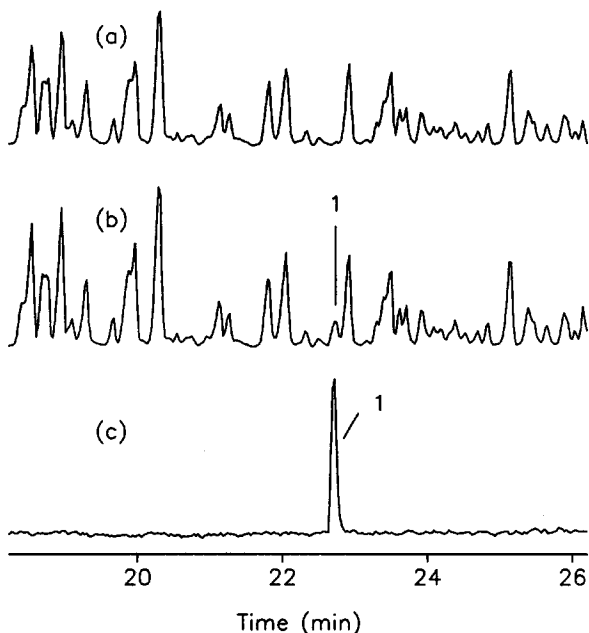


Fig. 9. Parallel FID and AFID chromatograms of gasoline. (a) FID chromatogram; (b) FID chromatogram of triethylphosphate (TEP) spiked into gasoline; peak 1 represents 5.1 ng of TEP; (c) parallel AFID chromatogram of b. GC conditions: column temperature: 30°C (1 min), 3°C/min to 185°C (5 min); split ratio of 150:1; 2- μ l injection.

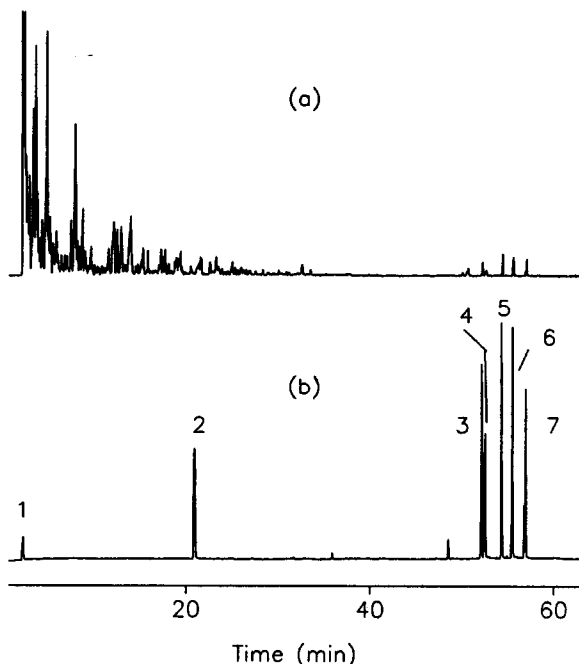


Fig. 10. Parallel chromatograms of gasoline spiked with six organophosphorus pesticides with (a) FID and (b) AFID. Peaks: 1 = acetone; 2 = TEPP 120 ng; 3 = phorate 141 ng; 4 = dimethoate 117 ng; 5 = disulfoton 118 ng; 6 = methyl parathion 210 ng; 7 = parathion 181 ng. GC conditions: column temperature: 50°C (1 min), 2°C/min to 140°C (10 min), 10°C/min to 240°C (8 min); split ratio of 50/1; 2 μ l injection volume.

ply shutting off the ultrasonic nebulizer and the nitrogen and hydrogen flows supplying the alkali salt flame. Fig. 9a is a segment of a capillary separation of a gasoline sample with FID detection, while the chromatograms in Fig. 9b and c illustrate the separation of gasoline spiked with triethylphosphate (peak 1 at 5.1 ng P). Fig. 9b is detected in the FID mode, while Fig. 9c illustrates the selectivity of the detector in the phosphorus mode. Further applications of detector selectivity are depicted in Fig. 10 of several organophosphorus pesticides spiked in gasoline and in Figs. 11 and 12 for commercial pesticide preparations in a complex matrix.

CONCLUSIONS

Although commercial FASD versions may offer improved detection limits and selectivity ratios, the linear range of this aerosol configura-

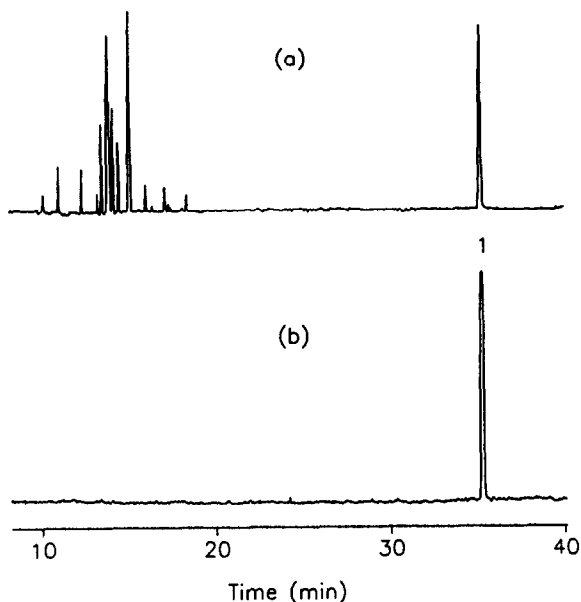


Fig. 11. Parallel chromatograms of a commercial Ortho diazinon preparation with (a) FID and (b) AFID. Peak 1 represents 36.8 ng P diazinon. GC conditions: column temperature: 40°C (5 min), 6°C/min to 250°C; split ratio of 150:1; 2- μ l injection of 1:10 dilution of preparation in acetone.

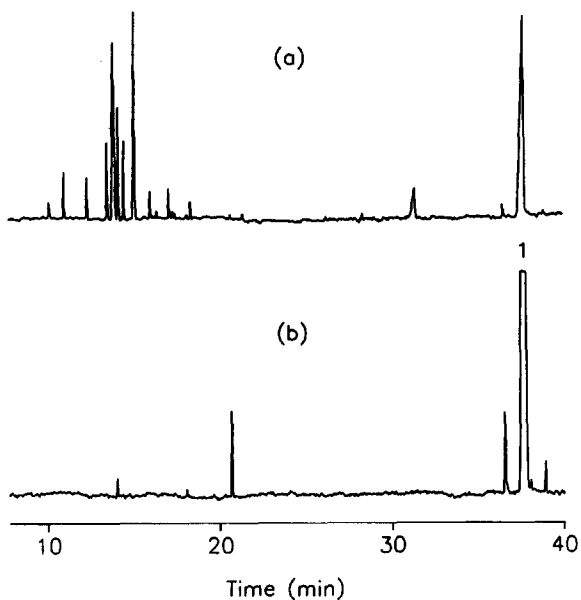


Fig. 12. Parallel chromatograms of a commercial Ortho malathion solution with (a) FID and (b) AFID. Peak 1 represents 75 ng P as malathion. GC conditions as in Fig. 11.

tion is comparable. In addition, modification to a FID is easily implemented by a simple pneumatic switching procedure. Moreover this detector offers several other advantages, which include no indication of fatigue and contamination with chlorinated solvents, and the ability to rapidly revert to the FID mode. In its present configuration, this detector offers considerable potential versatility, namely, by varying selectivity towards other heteratoms can be demonstrated.

ACKNOWLEDGEMENTS

E.D.C. wishes to acknowledge the Graduate School at University of Massachusetts Lowell for a research fellowship. The authors thank Galactic Industries for the gift of the LabCalc software and appreciate pesticide donations from Jetline Labs (Lowell, MA, USA), Revet Environmental and Analytical Laboratories (Worcester, MA, USA) and the Lawrence Experimental Station (Lawrence, MA, USA).

REFERENCES

- 1 A. Karmen and L. Giuffrida, *Nature*, 201 (1964) 1204.
- 2 L. Giuffrida, *J. Ass. Offic. Agr. Chem.*, 47 (1964) 293.
- 3 D.R. Coahran, *Bull. Environ. Contam. Toxicol.*, 1 (1966) 141.
- 4 K.P. Dimick, C.H. Hartmann, D.M. Oaks and E. Trone, *US Pat.*, 3 423 181 (1969).
- 5 H.C. Hartmann, *Bull. Environ. Contam. Toxicol.*, 1 (1966) 159.
- 6 H.C. Hartmann, *J. Chromatogr. Sci.*, 7 (1969) 163.
- 7 V.V. Brazhnikov and E.B. Shmidel, *J. Chromatogr.*, 122 (1976) 527.
- 8 G.R. Verga and F.J. Poy, *J. Chromatogr.*, 116 (1976) 17.
- 9 B. Kolb and J. Bischoff, *J. Chromatogr. Sci.*, 12 (1974) 625.
- 10 J.E. Baudean, *Can. Res. Dev.*, 8 (1975) 30.
- 11 C.A. Burgett and D.H. Smith, *J. Chromatogr.*, 134 (1977) 57.
- 12 P.L. Patterson, *J. Chromatogr.*, 167 (1978) 381.
- 13 P.L. Patterson and R.L. Howe, *J. Chromatogr. Sci.*, 16 (1978) 275.
- 14 P.L. Patterson, R.A. Gatten and C. Ontiveros, *J. Chromatogr. Sci.*, 20 (1982) 97.
- 15 J. Sevcik, *Chromatographia*, 6 (1973) 139.
- 16 V.V. Brazhnikov, M.V. Gur'ev and K.I. Sakodinskii, *Chromatographia*, 2 (1970) 53.
- 17 J. Carlson, *M.S. Thesis*, University of Lowell, Lowell, MA, 1981.
- 18 J.P. Foley and J.G. Dorsey, *Chromatographia*, 18 (1984) 503.